Remote Sens. **2015**, *7*, 15729-15747; doi:10.3390/rs71115729

OPEN ACCESS

remote sensing

ISSN 2072-4292

www.mdpi.com/journal/remotesensing

Article

Evaluation of Satellite and Reanalysis Soil Moisture Products over Southwest China Using Ground-Based Measurements

Jian Peng [1,*], Jonathan Niesel [1], Alexander Loew [1,2], Shiqiang Zhang [3] and Jie Wang [4]

1 Max Planck Institute for Meteorology, 20146 Hamburg, Germany;
E-Mails: jonathan.niesel@mpimet.mpg.de (J.N.); alexander.loew@lmu.de (A.L.)

2 Department of Geography, University of Munich (LMU), 80333 Munich, Germany

3 College of Urban and Environmental Sciences, Northwest University, Xi'an 710027, China;
E-Mail: zhangsq@lzb.ac.cn

4 Yunnan Institute of Water Resources and Hydropower Research, Kunming 650228, China;
E-Mail: wangjie@lzb.ac.cn

***** Author to whom correspondence should be addressed; E-Mail: jian.peng@mpimet.mpg.de;
Tel.: +49-89-2180-6515.

Academic Editors: Nicolas Baghdadi and Prasad S. Thenkabail

Received: 28 September 2015 / Accepted: 18 November 2015 / Published: 23 November 2015

Abstract: Long-term global satellite and reanalysis soil moisture products have been available for several years. In this study, *in situ* soil moisture measurements from 2008 to 2012 over Southwest China are used to evaluate the accuracy of four satellite-based products and one reanalysis soil moisture product. These products are the Advanced Microwave Scanning Radiometer for the Earth observing system (AMSR-E), the Advanced Scatterometer (ASCAT), the Soil Moisture and Ocean Salinity (SMOS), the European Space Agency's Climate Change Initiative soil moisture (CCI SM), and the European Centre for Medium-Range Weather Forecasts (ECMWF) Interim Reanalysis (ERA-Interim). The evaluation of soil moisture absolute values and anomalies shows that all the products can capture the temporal dynamics of *in situ* soil moisture well. For AMSR-E and SMOS, larger errors occur, which are likely due to the severe effects of radio frequency interference (RFI) over the test region. In general, the ERA-Interim (R = 0.782, ubRMSD = 0.035 m^3/m^3) and CCI SM (R = 0.723, ubRMSD = 0.046 m^3/m^3) perform the best compared to the other products. The accuracy levels obtained are comparable to validation results from other regions. Therefore, local hydrological applications and water resource management will benefit from the long-term ERA-Interim and CCI SM soil moisture products.

Keywords: validation; *in situ* soil moisture; satellite-based soil moisture; reanalysis soil moisture; Southwest China

1. Introduction

Soil moisture (SM) plays an important role in the interactions between the atmosphere and the land surface, and has been identified as an essential climate variable by the Global Climate Observing System (GCOS) [1]. Soil moisture connects the energy and water fluxes due to its control on the partitioning of surface net energy into latent and sensible heat fluxes, as well as the partitioning of precipitation into infiltration and runoff [2,3]. Therefore, the knowledge of soil moisture dynamics is important for climate change research, flood and drought monitoring, weather forecasting, as well as water resource management [4,5].

Satellite remote sensing has been recognized as a powerful tool to retrieve soil moisture due to the improvements of sensor technologies and retrieval algorithms [6] using either active [7] or passive microwave [8] remote sensing observations. Until now, several global satellite-based soil moisture products have been released. These products include the Advanced Microwave Scanning Radiometer E for the Earth observing system (AMSR-E) [9], the Advanced Scatterometer (ASCAT) [10,11], the Soil Moisture and Ocean Salinity (SMOS) [12], and the European Space Agency's Climate Change Initiative (ESA CCI) soil moisture product [13–15]. These satellite-based soil moisture products provide an unprecedented opportunity to investigate the interactions between land and atmosphere and their effects on climate change. However, comprehensive evaluations of these soil moisture products are required before using them. Many evaluation studies have been conducted either based on *in situ* measurements or model simulations. Most of these studies are performed either on a regional scale, for example in Europe [16–19], Australia [20,21], Africa [22,23], and the United States [24,25], or at the global scale [15,26,27]. However, few studies were conducted in China so far. In order to utilize the satellite-based soil moisture products for practical applications in China, it is necessary to validate them against *in situ* measurements in China.

The objective of this research is to evaluate four satellite-based soil moisture products and one reanalysis product with *in situ* measurements over Yunnan, China (Figure 1). The validation activity is of great importance, because this region is very sensitive and vulnerable to climate change due to its unique geophysical position and climate. Over the last three decades, frequent droughts and floods occurred in this region, with the most extreme drought occurring from winter 2009 to spring 2010 [28,29]. According to the Ministry of Civil Affairs, the drought resulted in a loss of $2.5-billion due to agricultural damage, and about 9.65 million people have had a shortage of drinking water [30]. Therefore, accurate long-term satellite-based soil moisture products are urgently required to assess drought conditions and the links between increasing temperature, soil moisture variations, and vegetation productivity. The following section briefly introduces the study area, *in situ* measurements, and soil moisture products. The evaluation methods are described in Section 3. Results of the evaluation are then presented and discussed in Section 4. Finally, conclusions are summarized in Section 5.

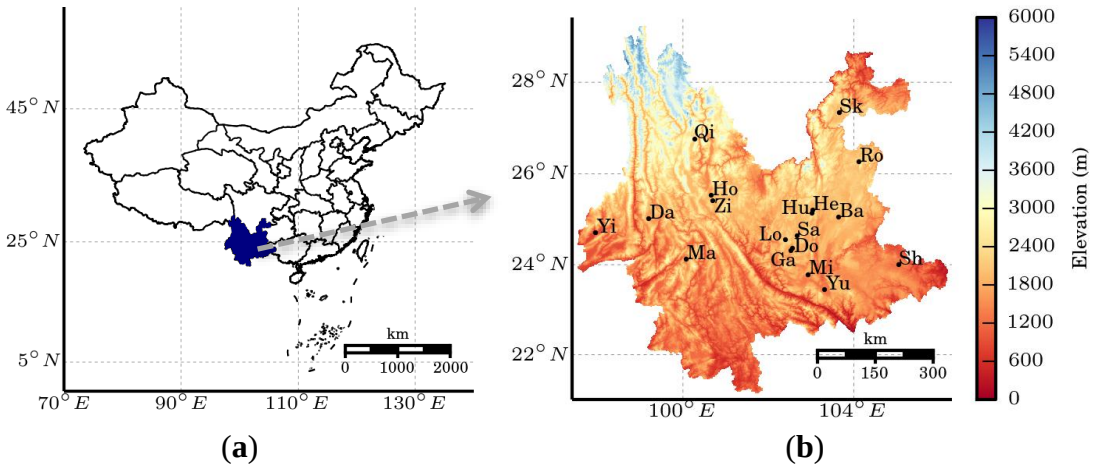

Figure 1. Study area in Southwest China (**a**) and locations of *in situ* soil moisture stations (**b**).

2. Study Area

The Yunnan province is located in Southwest China (Figure 1), covering an area of roughly 394,000 km^2. Mountainous topography and special karst geomorphology characterize this region, with an elevation gradually decreasing from the northwest to southeast, and an average elevation of 1980 m above sea level [31]. This region has a subtropical climate with dry winters and wet summers. The precipitation is spread unevenly over the year and the region, and is largely influenced by the Tibetan plateau, the tropical Indian monsoon and the eastern Asia monsoon. As a result, about half of the precipitation occurs between June and August. The annual precipitation ranges from 600 mm in valleys to 1700 mm in mountainous regions [32,33]. Due to its special climate and topographical conditions, this region suffers from frequent droughts. The most severe and sustained drought occurred in 2010. It started in the winter of 2009 and became particularly severe in the spring of 2010, leading to significant ecological and economic damages [34]. Numerous streams and small reservoirs dried up, which had a severe impact on the supply of drinking water and the agricultural production [30,35]. Therefore, long-term and spatially distributed soil moisture information is required for this region.

3. Materials and Methods

3.1. Satellite-Based and Reanalysis Products

The satellite products used in this study include four soil moisture products as well as one precipitation product. In addition, one soil moisture reanalysis product is also analyzed. In the following subsections, these datasets are briefly introduced.

3.1.1. AMSR-E

The AMSR-E onboard the Aqua satellite is a passive microwave sensor. The instrument operated between May 2002 and October 2011. It provided measurements at six different frequencies. Data is available for descending (1:30 a.m.) and ascending (1:30 p.m.) orbits [36]. Several algorithms have been developed for retrieving soil moisture from the AMSR-E measurements. One of them is the land parameter retrieval model (LPRM) [9]. The corresponding soil moisture product has been developed and

released by Vrije Universiteit Amsterdam (VUA) together with NASA. The LPRM product provides global soil moisture on a regular 0.25 °global grid derived from C-band and X-band observations. The observations from the X-band are used only for soil moisture estimation when the C-band observations are affected by radio frequency interference (RFI). Based on the observations from these two bands at two overpass times, the LPRM product contains four soil moisture products (C-band and X-band soil moisture in both, in descending and ascending modes). In this study, all these products were compared with *in situ* measurements to investigate their performance using the period from 2008 to 2011. The soil moisture data were masked if the vegetation optical depth (VOD) was higher than 0.8, as suggested by Rebel *et al.* [37] and Lei *et al.* [38].

3.1.2. ASCAT

The ASCAT is a scatterometer onboard the Meteorological Operation-A (MetOp-A) satellite, which was launched in October 2006 and scans the Earth's surface in descending (9:30 a.m.) and ascending (9:30 p.m.) orbits [39]. It operates in the C-band (5.3 GHz) in vertical polarization with a spatial resolution of 25 or 50 km [40]. The soil moisture is derived from the backscatter measurements of ASCAT using a change detection algorithm [11]. In this study, the soil moisture product provided by the European Organization for the Exploitation of Meteorological Satellites (EUMETSAT) with the version of TU-Wien-WARP 5.5 was used. It provides a relative soil moisture saturation degree (using the top 2 cm of the soil column) with values ranging from 0% (dry) to 100% (wet) at spatial resolution of 25 km. To be consistent with *in situ* soil moisture measurements and comparable with other soil moisture products, the ASCAT soil moisture was rescaled into volumetric soil moisture (unit: m^3/m^3) using the soil porosity estimated from Land Data Assimilation System (LDAS) data [41]. The soil moisture products from 2008 to 2012 in both descending and ascending modes were analyzed in this study. The soil moisture data were masked if the processing flags were not equal to 0 (best quality).

3.1.3. ESA CCI

The ESA CCI soil moisture product is a unique 35-year (1978–2013) long satellite-based soil moisture record produced within the framework of the ESA Climate Change Initiative [42]. The CCI soil moisture was generated by merging several passive and active soil moisture products [13,43]. The involved soil moisture products are derived from Scanning Multichannel Microwave Radiometer (SMMR), Special Sensor Microwave/Imager (SSM/I), Tropical Rainfall Measuring Missions (TRMM) Microwave Imager (TMI), ASMR-E, scatterometers (SCAT) and ASCAT. The CCI soil moisture has three products, which differ in the data sources used: passive microwave only, active microwave only, and merged passive-active product [15]. In this study, the merged passive-active product (version 02.1) is analyzed for the period from 2008 to 2012. The dataset has spatial resolution of 0.25 °on a daily basis.

3.1.4. SMOS

The SMOS satellite, launched in November 2009, is dedicated to soil moisture monitoring with an L-band (1.4 GHz) passive radiometer. It provides global coverage every three days for both descending (6:00 p.m.) and ascending (6:00 a.m.) orbits with a spatial resolution of about 40 km [44]. The advantage

of the L-band is that it has greater sensing depth of up to 5 cm of the soil. The soil moisture is derived using the L-band microwave emission of the biosphere (L-MEB) model [45,46]. In this study, the SMOS level 3 daily soil moisture product was obtained from the Centre Aval de Traitement des Données SMOS (CATDS). As is the case for AMSR-E and ASCAT, both descending and ascending soil moisture products were used for analysis from the years from 2009 to 2012. According to Al-Yaari *et al.* [47], the soil moisture data are masked out if the Data Quality Index (DQX) is larger than 0.06, or the DQX is equal to 0 (filled value), or the RFI is larger than 30%.

3.1.5. ERA-Interim

ERA-Interim is a global atmospheric reanalysis product produced by the ECMWF [48]. It is based on a sequential data assimilation scheme. It covers the period from 1979 until the present. The soil moisture data from ERA-Interim are provided at four depths (0–7, 7–28, 28–100, and 100–289 cm) [48]. In this study, the daily averaged 0.25 °upper layer (0–7 cm) of soil moisture products covering the years from 2008 to 2012 were evaluated.

3.1.6. TRMM Precipitation Data

The TRMM precipitation data was used in this study as an alternative to the station precipitation from *in situ* measurements, because it has been extensively validated against ground-based measurements around the world, including the Yunnan province [33]. Details of the TRMM precipitation dataset can be found in Kummerow *et al.* [49] and Iguchi *et al.* [50]. The daily 0.25 °TRMM precipitation products (3B42 V7) were used in this study for the same period as indicated in the other dataset (2008–2012).

3.2. In Situ Soil Moisture Measurements

There are a total of 18 soil moisture stations used in the current study. The geographical locations and details of these stations are presented in Figure 1 and Table 1. The elevations of these stations range from 847 m to 2293 m, and the land cover types are mainly grassland (4 stations), forest (3 stations), cropland (7 stations), and bare soil (4 stations). The soil moisture contents over these stations were measured at three different depths (10 cm, 20 cm and 40 cm) using frequency domain reflectometry (FDR) sensors. Data was obtained from the Yunnan Hydrology and Water Resources Bureau. The measurements at a 10 cm depth are considered to best represent the soil layer accessible by the satellite observations. We therefore use this layer as a reference in this study.

Table 1. Descriptions of the *in situ* soil moisture stations used in the study.

Station Name	Short Name	Land Use	Latitude (°)	Longitude (°)	Elevation (m)
Daciping	Da	Cropland	25.02	99.20	1685
Zijin	Zi	Bare soil	25.42	100.70	1958
Hongqi	Ho	Grassland	25.53	100.67	2044
Yingjiang	Yi	Bare soil	24.70	97.95	847
Yuguopu	Yu	Cropland	23.45	103.32	1283

Table 1. *Cont.*

Station Name	Short Name	Land Use	Latitude (°)	Longitude (°)	Elevation (m)
Mianyangchong	Mi	Forest	23.78	102.93	1433
Sanduo	Sa	Grassland	24.64	102.67	1967
Longwangtang	Lo	Forest	24.55	102.40	2099
Heyou	He	Cropland	25.20	103.03	1968
Huangjiapo	Hu	Grassland	25.13	103.02	2140
Qiaotou	Qi	Cropland	26.77	100.27	2293
Mayidui	Ma	Cropland	24.12	100.07	1344
Bamaochong	Ba	Grassland	25.05	103.63	1857
Rongfeng	Ro	Bare soil	26.26	104.11	1973
Shaba	Sh	Forest	24.00	105.05	1415
Dongfeng	Do	Bare soil	24.37	102.57	1653
Gaocang	Ga	Cropland	24.32	102.52	1650
Sankeshu	Sk	Cropland	27.33	103.67	1909

3.3. Evaluation Strategies

In order to evaluate the performances of the satellite-based and reanalysis soil moisture products, they were first compared directly with the *in situ* soil moisture. Established skill scores, like the correlation coefficient (R), the BIAS, the root mean square difference (RMSD), and the unbiased RMSD (ubRMSD) were used to quantify the differences between various soil moisture products and measured soil moisture [51,52]. In addition, the comparisons for soil moisture anomalies were also performed, because the seasonal variations of soil moisture may influence the correlation statistics [53]. The soil moisture anomalies were computed similar to Dorigo *et al.* [15], using the equation below to avoid the seasonal effects on correlations. The anomaly calculation is based on a sliding window of five weeks. The difference from the mean is calculated if there are at least five measurements available during this time window.

$$Anom(t) = SM(t) - \overline{SM(t-17:t+17)} \quad (1)$$

where SM(t) is the soil moisture at day t, the overbar indicates the temporal mean for the five weeks period. Based on the above equation, the soil moisture anomalies of *in situ* soil moisture, satellite-based, and reanalysis products were calculated.

4. Results and Discussion

4.1. Direct Comparison of Soil Moisture

4.1.1. Pre-Selection of Best Performed AMRS-E, ASCAT, and SMOS

From direct comparisons with *in situ* soil moisture, it is found that the AMSR-E X-band has better performance than the C-band with lower RMSD and ubRMSD values. It implies that the C-band observations might be influenced by the RFI in this region. Regardless of the frequency band, ascending and descending soil moisture products also have different accuracies due to the diurnal variations of the land surface conditions. On one hand, overpass times at night and in the early morning are more suitable for soil moisture retrieval from passive microwave satellites, because the isothermal conditions at night

can minimize the errors associated with surface temperature [54]. On the other hand, the soil emission is influenced by the diurnal variation of the water in the vegetation canopy [55]. The attenuation of soil emission caused by water in the vegetation canopy is minimized during the daytime due to loss of water through evapotranspiration [56]. Therefore, both daytime and nighttime retrievals have certain advantages. For AMSR-E, many studies such as Brocca *et al.* [17] have found that ascending soil moisture is more reliable than descending soil moisture. However, in other studies such as Griesfeller *et al.* [57], descending was found to be better than ascending. This demonstrates that the performance of different AMSR-E soil moisture products depends on the surface condition of the study area. In this study, it is found that ascending AMSR-E performs better than descending AMSR-E, which might be due to the heavily vegetated characteristics of the study area. Similar results have been reported by Lei *et al.* [38], who found that the advantage of the nighttime overpass is reduced as the vegetation cover increases and the AMSR-E ascending retrieval is superior over heavily vegetated areas in the United States. Therefore, the descending and ascending soil moisture products should be evaluated before applying them in different regional studies. Compared to AMSR-E, the differences between ascending and descending retrievals are smaller for SMOS. It may be due to the smaller soil moisture temperature differences between ascending/descending overpass times of SMOS than that of AMSR-E. The Faraday rotation effect in the ionosphere is also expected to be minimized at SMOS ascending overpass time [38]. Although SMOS ascending performs slightly better than descending, the sample days of SMOS ascending soil moisture are less than descending soil moisture in the current study. Therefore, the SMOS descending soil moisture is used for the following analyses. Compared to AMSR-E and SMOS, the ASCAT presents quite similar performance for ascending and descending soil moisture. This is partly because the scatterometer-based ASCAT does not require accurate estimates of surface temperature [38]. It is worth noting that the ASCAT descending soil moisture has slightly better correlation values than ascending soil moisture in the current study area. The statistics of the above comparisons are provided in Appendix Figure A1. In the following analyses, only the best performed AMSR-E ascending X band (AMSR-E_A_X), ASCAT descending (ASCAT_D), and SMOS descending (SMOS_D) are considered in comparisons with *in situ* measurements.

4.1.2. Temporal Evolution of Soil Moisture and Precipitation

Figure 2 shows the time series patterns of all the soil moisture products, *in situ* measurements and rainfall for the average values over all stations. All the products except for AMSR-E and SMOS correspond well with rainfall, with the soil moisture increasing during rainfall events and decreasing after rainfall events. Additionally, the temporal dynamics of *in situ* soil moisture are captured well by CCI SM and ERA-Interim. It can also be seen that CCI SM and ERA-Interim, which are in line with *in situ* measurements, capture the spring droughts in 2010. Compared to *in situ* soil moisture, the ASCAT has higher seasonal variability. The poor performance of AMSR-E and SMOS might be due to the effects of RFI over this region, because both AMSR-E and SMOS are reported to correlate well with ground-based measurements over other regions, such as America, West Africa, and Europe [23,25,26].

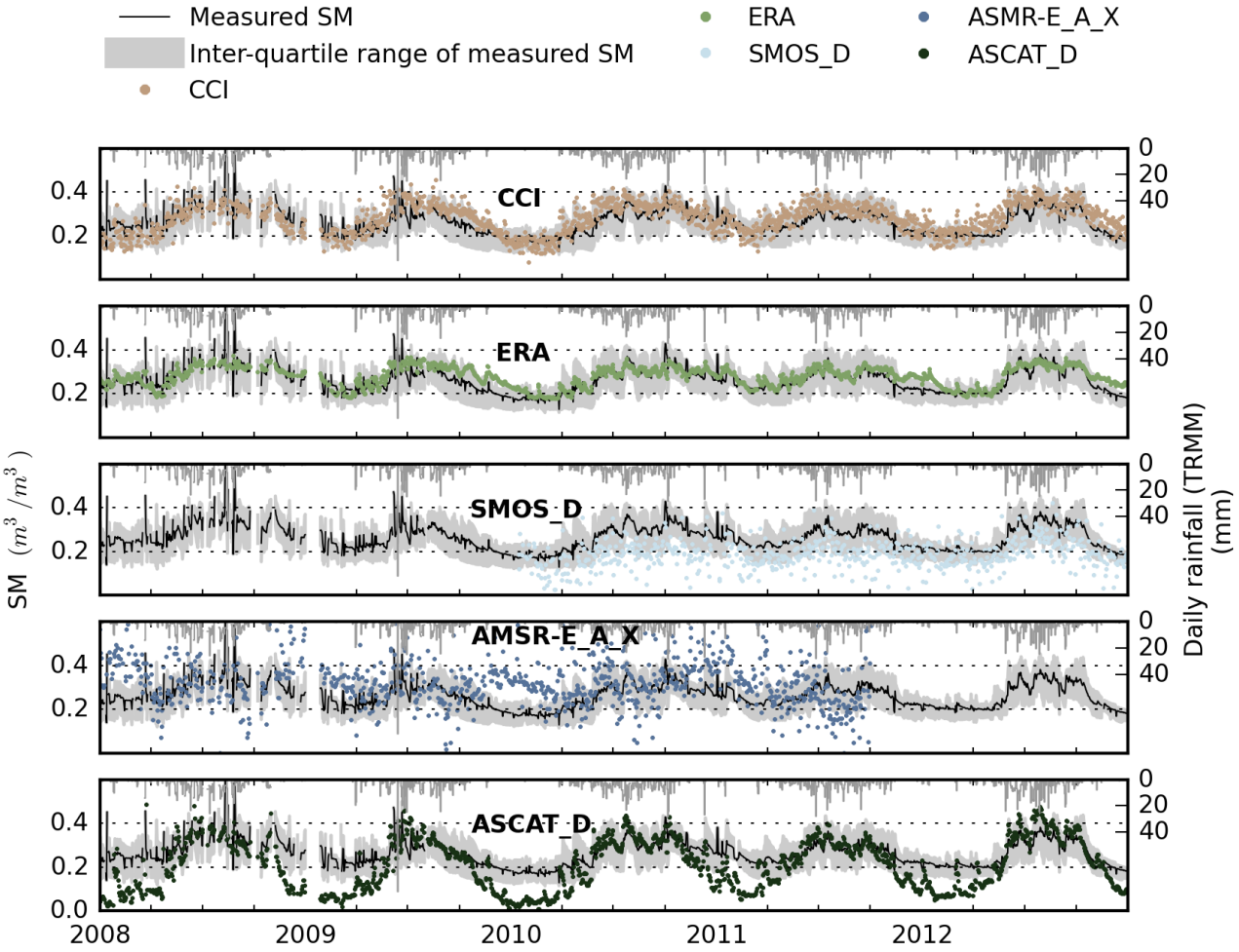

Figure 2. Temporal evolution of the averaged *in situ* measurements, soil moisture products, and precipitation at network scale: *in situ* mean soil moisture (black solid line) and its inter-quartile range (grey shaded areas); European Space Agency's Climate Change Initiative (CCI), Interim Reanalysis (ERA), Soil Moisture and Ocean Salinity (SMOS), Advanced Microwave Scanning Radiometer for the Earth observing system (AMSR-E)_A_X and Advanced Scatterometer (ASCAT)_D (points with different color); and precipitation (top of each panel). The soil moisture has the unit of m^3/m^3 (left y-axis), while precipitation has the unit of mm (right y-axis).

4.1.3. Validation of the Soil Moisture against *in Situ* Measurements

To quantitatively evaluate these soil moisture products, Figure 3 shows the comparison statistics between different soil moisture products and *in situ* measured soil moisture at each station. In general, the ASCAT, CCI SM, and ERA-Interim have similar R values. However, in terms of RMSD and ubRMSD, the best performance was found with the ERA-Interim, followed by CCI SM and ASCAT. It can also be seen that the accuracies of AMSR-E and SMOS are much worse than the expected accuracy of 0.06 $m^3\ m^{-3}$ for AMSR-E and 0.04 $m^3\ m^{-3}$ for SMOS. In theory, the SMOS should provide reliable soil moisture product due to the use of L-band measurements. As stated before, the poor performance

found here might be caused by the effects of RFI. Similar results have been reported by Cho *et al.* [58] and Zeng *et al.* [59].

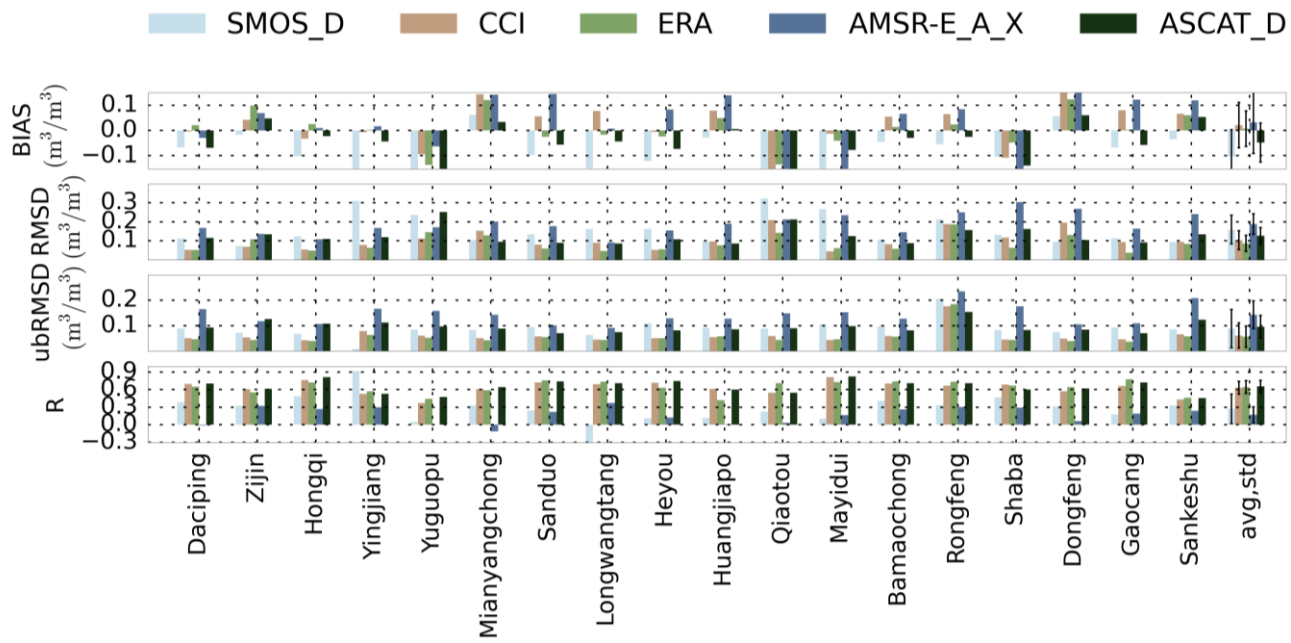

Figure 3. Bar plots of the comparison results between soil moisture products and *in situ* measurements at each station.

In addition to the validation at each individual station, the comparisons between averaged *in situ* soil moisture over all stations and corresponding averaged soil moisture products were also conducted. This comparison method is expected to reduce the uncertainties introduced by scale differences between the *in situ* point and satellite pixel [60]. Table 2 presents the statistical scores of the comparison results at the network scale. Compared to the results at station scale, the comparisons at the network scale generally show the same tendency but better scores. The ERA-Interim outperforms other soil moisture products with lowest RMSD and ubRMSD.

Table 2. Statistics of comparisons between averaged *in situ* soil moisture and soil moisture products at network scale.

Products	R	BIAS (m^3/m^3)	RMSD (m^3/m^3)	ubRMSD (m^3/m^3)	Sample Days
CCI	0.723	0.019	0.050	0.046	1621
ERA	0.782	0.014	0.037	0.035	1692
AMSR-E_A_X	0.086	0.067	0.152	0.136	965
ASCAT_D	0.778	−0.053	0.096	0.080	1686
SMOS_D	0.443	−0.074	0.096	0.062	657

4.2. Comparison of Soil Moisture Anomalies

4.2.1. Temporal Evolution of Soil Moisture and Precipitation

The above results give an overview of the evaluation of soil moisture absolute values. To remove the influences of the seasonal cycle in the comparison, the soil moisture anomalies were calculated based

on Equation (1). Figure 4 shows the anomaly time series of the soil moisture and rainfall products. The CCI SM, ASCAT, and ERA-Interim generally represent the variations of *in situ* measurements. As expected, AMSR-E and SMOS have large variations compared to *in situ* soil moisture. Together with the analysis of the absolute soil moisture time series, these results suggest that *in situ* soil moisture temporal variations can be well represented by the satellite-based soil moisture and reanalysis datasets.

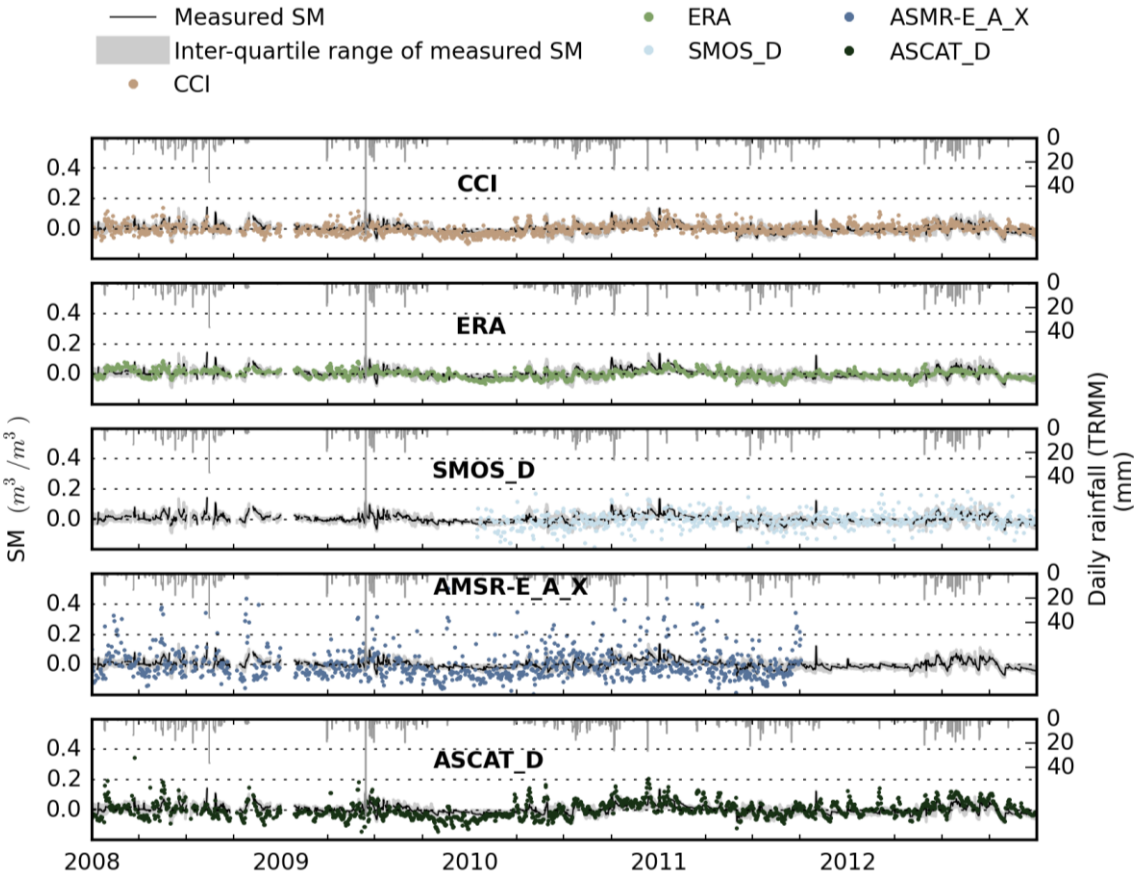

Figure 4. Temporal evolution of the anomalies from averaged *in situ* measurements, soil moisture products, and precipitation at the network scale: *in situ* mean soil moisture (black solid line) and its inter-quartile range (grey shaded areas); CCI, ERA, SMOS, AMSR-E_A_X, and ASCAT_D (points with different colors); and precipitation (top of each panel). The soil moisture has the unit of m^3/m^3 (left y-axis), while precipitation has the unit of mm (right y-axis).

4.2.2. Validation of the Soil Moisture Anomalies

Figure 5 presents the bar plots of the comparison of soil moisture anomalies at each station. Similar to the results from the comparison of absolute soil moisture, the CCI SM, ASCAT, and ERA-Interim have similar performance in terms of R values. As expected, the R values are smaller than that of absolute comparison due to the removal of seasonal cycles. Similar results have been reported by Albergel *et al.* [16] and Brocca *et al.* [17]. However, the RMSD, ubRMSD, and BIAS values of anomaly comparisons are smaller than that of the absolute comparisons. The ERA-Interim has the smallest RMSD, ubRMSD, and BIAS. Similar performance was found with CCI SM, followed by ASCAT. The AMSR-E and SMOS have the worst performance.

The statistic scores of the comparison of soil moisture anomalies at a network scale are summarized in Table 3. Due to the decreasing of uncertainties of scale difference, the scores of network scale are improved compared to that of the station scale. In comparison to the scores of absolute soil moisture (Table 2), the correlations of all the products worsen, while RMSD, ubRMSD, and BISA get smaller. In general, the ERA-Interim has the smallest RMSD and ubRMSD, which indicates that the ERA-Interim agrees best with *in situ* soil moisture. The performance of CCI SM is comparable with the ERA-Interim soil moisture.

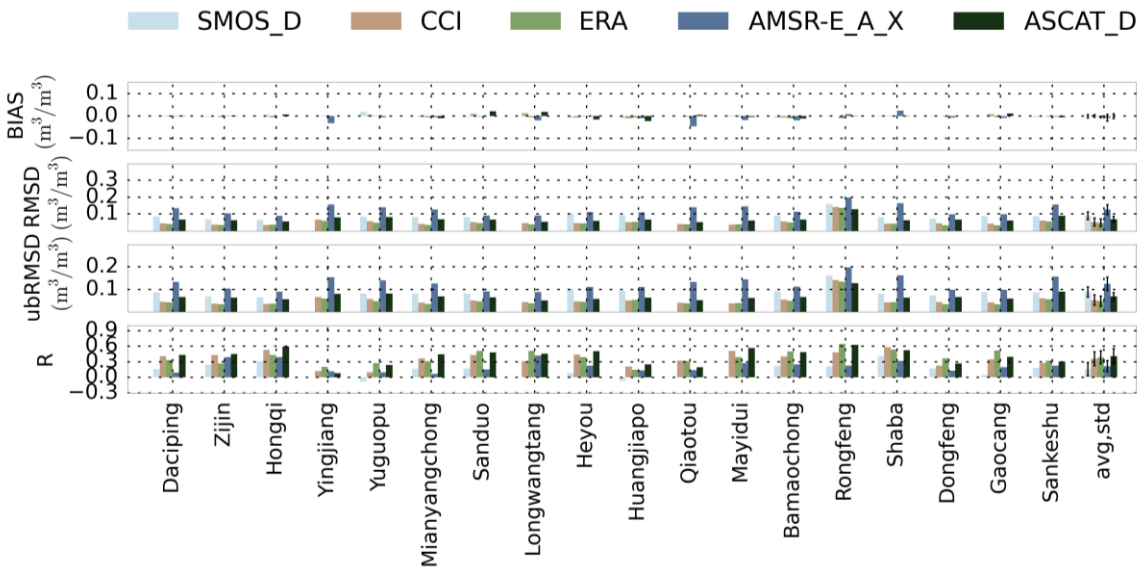

Figure 5. Bar plots of the results from anomalies comparison between soil moisture products and *in situ* soil moisture at each station.

Table 3. Statistics of the anomalies comparison between averaged *in situ* soil moisture and soil moisture products at network scale.

Products	R	BIAS (m^3/m^3)	RMSD (m^3/m^3)	ubRMSD (m^3/m^3)	Sample Days
CCI	0.480	−0.002	0.030	0.030	1621
ERA	0.634	−0.003	0.023	0.023	1692
AMSR-E_A_X	0.222	−0.007	0.101	0.101	962
ASCAT_D	0.564	−0.004	0.044	0.044	1686
SMOS_D	0.303	−0.004	0.054	0.054	656

4.2.3. Seasonal and Land Cover Analysis

Furthermore, the seasonal analysis was conducted to identify any seasonal variations of the dataset accuracies. The study period is separated into four seasons September/October/November (autumn), December/January/February (winter), March/April/May (spring), and June/July/August (summer) respectively. It can be seen from Figure 6 that all products have small variations over different seasons in terms of R, RMSD, and ubRMSD values. This indicates that the accuracy of these soil moisture products is stable in different seasons.

In addition, the influence of land use on the statistical scores was also examined. The stations are divided into four land use groups: bare soil (4), cropland (7), forest (3), and grassland (4). The results were shown in Figure 7. In general, different land use categories have similar performance in terms of statistical

scores for all the products except SMOS. SMOS has very low R value over cropland. These results suggest that the performance of soil moisture products is generally insensitive to land use.

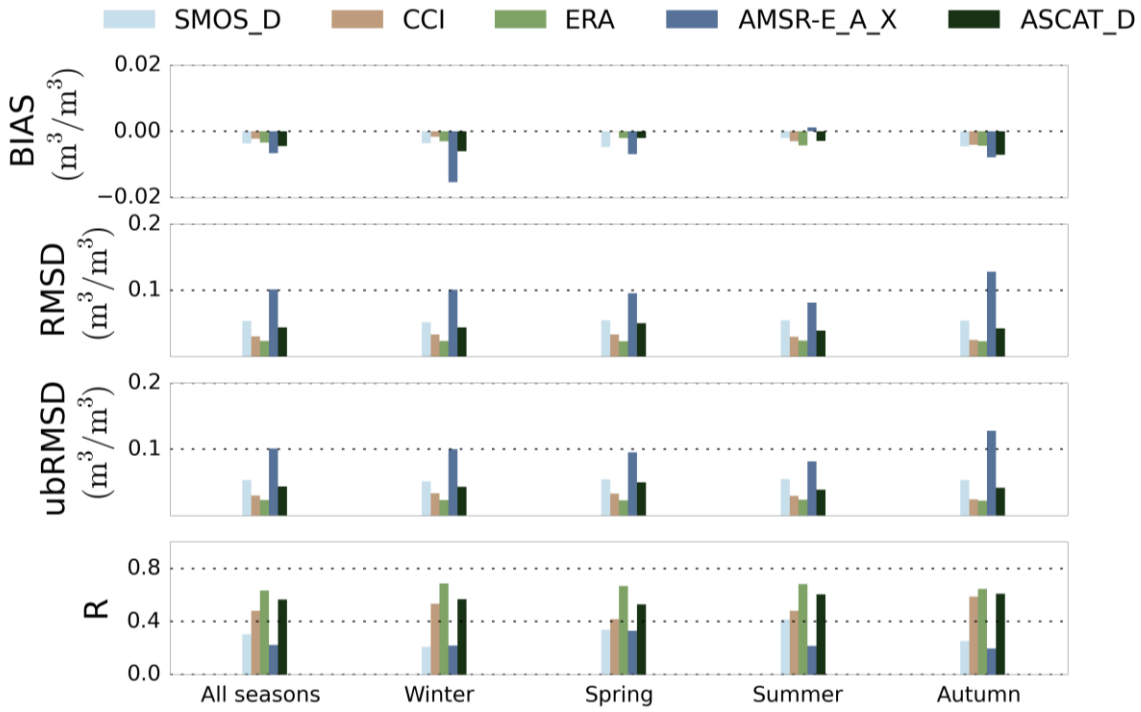

Figure 6. Bar plots of the comparison results between soil moisture products and *in situ* measurements over different seasons.

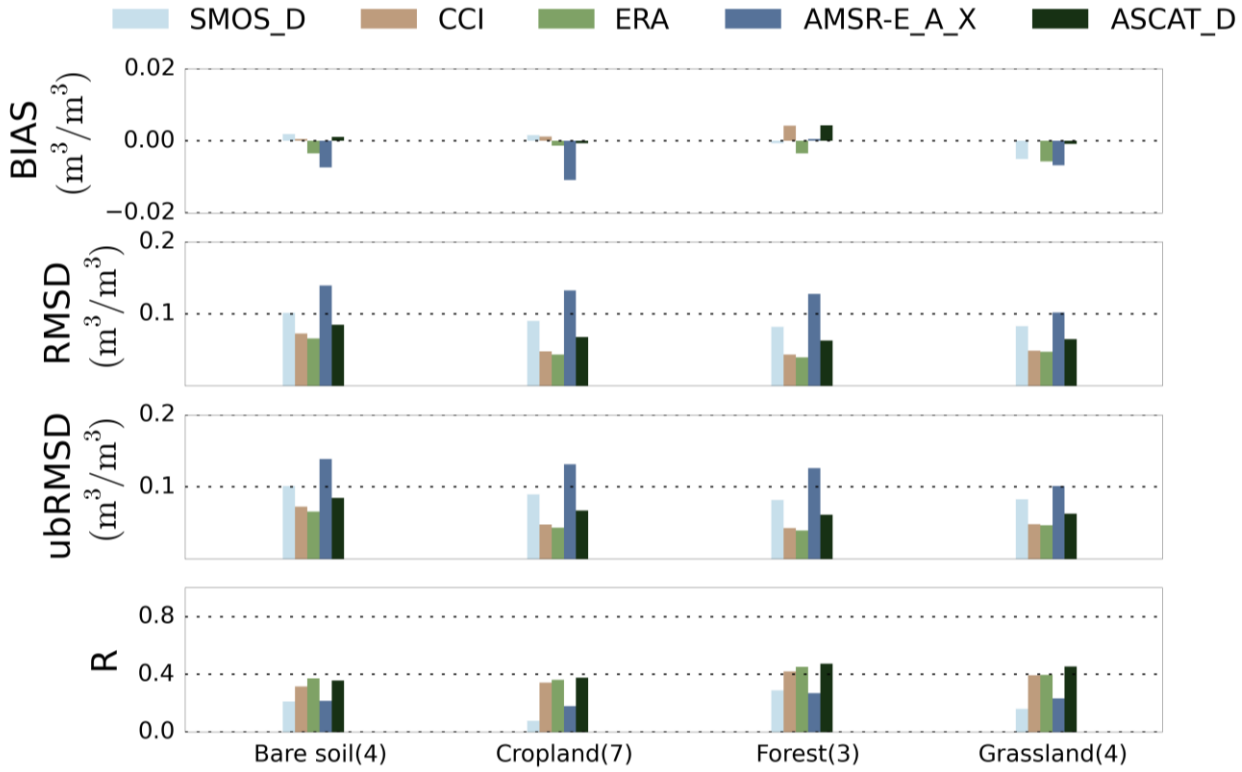

Figure 7. Bar plots of the comparison results between soil moisture products and *in situ* measurements over different land cover types.

4.3. Discussion

This study examined the ability of several soil moisture products to represent the surface soil moisture conditions over Yunnan, China. The results highlight the performance of ERA-Interim and CCI SM. From the time series analysis of both absolute values and anomalies, it is found that ERA-Interim and CCI SM can capture the variations of *in situ* soil moisture and respond well to the rainfall events. From quantitative comparison with *in situ* measurements, the ERA-Interim has the lowest RMSD and ubRMSD. The CCI SM has comparable performance to ERA-Interim. The accuracy levels are also similar to that reported by validation studies over other regions [59,61,62]. Additionally, the seasons and land use have little effect on the performance of these products. This indicates that both ERA-Interim and CCI SM have the potential to benefit the local hydrological applications such as drought monitoring, and water planning and management.

The unfavorable results of AMSR-E and SMOS are very likely due to the affects of RFI. The RFI disturbs the natural microwave emission observed by SMOS, leading to the unreliable estimation of soil moisture. The impacts of RFI on SMOS and AMSR-E have been found in Western Europe, Northeast Asia, and Middle East [58,63]. The present study further indicates the strong impacts of RFI on SMOS and AMSR-E in Southwest China.

Although most of the soil moisture can represent the surface soil moisture, there are still several issues that need to be addressed in future studies: (I) the scale mismatch between satellite pixel and *in situ* point; (II) the mismatch between the satellite penetration depth and *in situ* measurement depth; (III) the inaccuracies of the input data (such as land surface temperature and soil texture) for the soil moisture retrieval; and (IV) the improvement of the retrieval algorithms.

In addition to the improvement of soil moisture retrieval accuracy, there is also a need to improve the spatial resolution of the soil moisture product. The current global soil moisture products normally have spatial resolutions of tens of kilometers. However, many regional hydrological applications require a spatial resolution of 1–10 km [64,65]. The optical/thermal infrared (TIR) sensors can provide complementary information of soil moisture at higher spatial resolutions. Therefore, the synergistic use of microwave and optical/thermal data to estimate soil moisture at high spatial resolution should be another direction in future study.

5. Conclusions

Validation of satellite-based soil moisture products is essential at both the regional and global scale. The present study evaluated four satellite-based and one reanalysis soil moisture product over an intensive soil moisture network in Southwest China. The results show that these products can capture well the seasonal variations of *in situ* soil moisture. Larger deviations were observed in particular for AMSR-E and SMOS products. The SMOS underestimates soil moisture, while AMRS-E overestimates soil moisture. The biases of AMSR-E and SMOS are very likely due to the strong radio frequency interference (RFI) that affects the measurements in this region. Quantitative validations show that ERA-Interim ($R = 0.782$, ubRMSD = 0.035 m^3/m^3) and CCI SM ($R = 0.723$, ubRMSD = 0.046 m^3/m^3) outperform the other products. In addition, these soil moisture products were found to provide similar performance across the year and for different landcover types. No systematic differences in soil moisture

accuracy could be identified throughout the different seasons. Due to their long-term coverage (1978–2013 for CCI SM, 1979—present for ERA-Interim), the CCI SM and ERA-Interim dataset have the potential to provide valuable information for hydrological applications and water resource management applications in the future.

Acknowledgments

The authors would like to acknowledge Yunnan Hydrology and Water Resources Bureau for providing the *in situ* soil measurements. The authors also would like to thank the Integrated Climate Data Centre (ICDC), Centre Aval de Traitement des Donn ées SMOS (CATDS), the European Space Agency (ESA), and the European Centre for Medium-Range Weather Forecasts (ECMWF) for providing the satellite-based and reanalysis soil moisture products. Additionally, Gitta Lasslop was acknowledged for reviewing the first version of the manuscript. Authors are also grateful to the three anonymous reviewers for their constructive comments and suggestions that helped improving the manuscript. This research was supported by the Cluster of Excellence CliSAP (EXC177), University of Hamburg, funded through the German Science Foundation (DFG), and the ESA CCI program (CMUG), and the project of Yunnan Social Development (2012CA021).

Author Contributions

Jian Peng designed the research, analyzed the results, and wrote the manuscript. Jonathan Niesel performed the research. Alexander Loew designed and supervised the research. Shiqiang Zhang and Jie Wang processed the *in situ* measurements.

Conflicts of Interest

The authors declare no conflict of interest.

Appendix

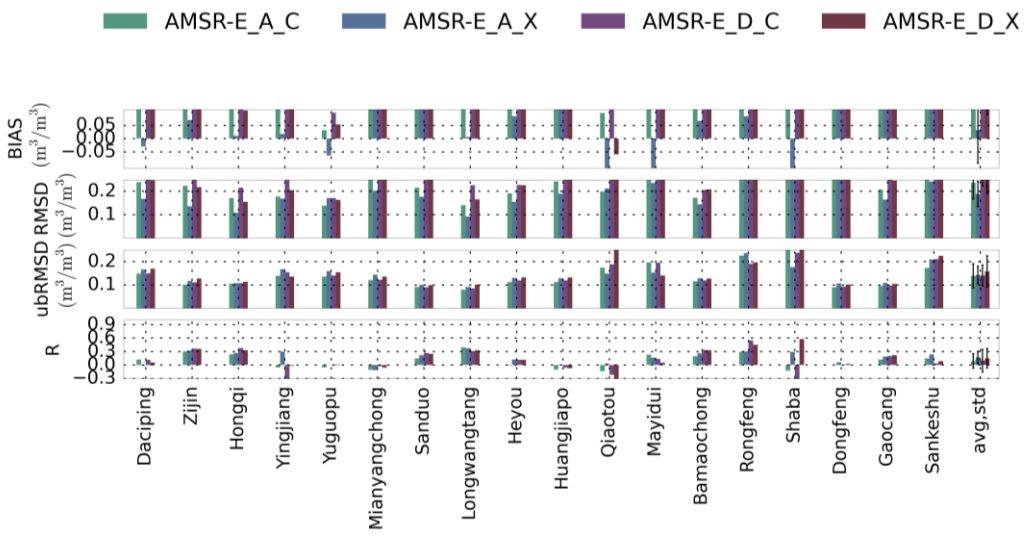

(**a**)

Figure A1. *Cont.*

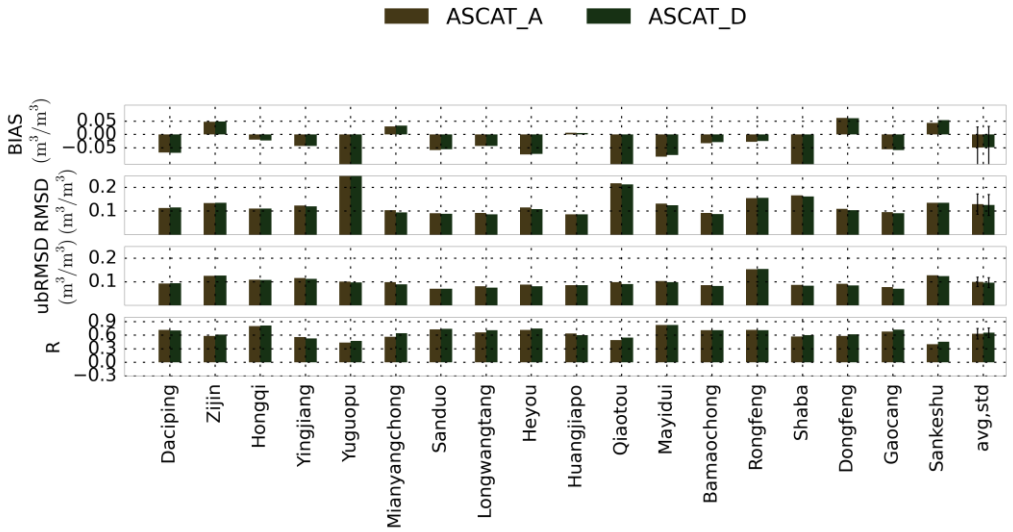

(**b**)

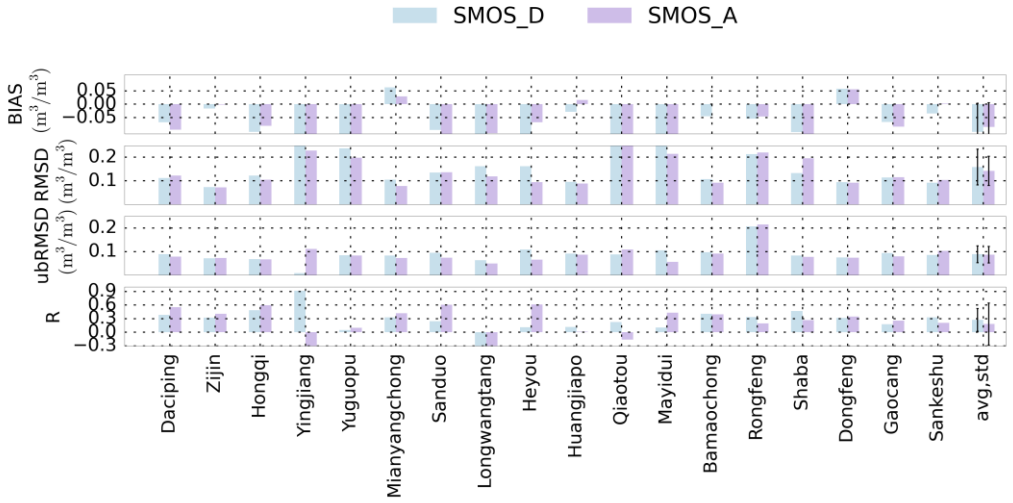

(**c**)

Figure A1. Bar plots of the comparison results between *in situ* measurements and soil moisture products: (**a**) AMSR-E; (**b**) ASCAT; (**c**) SMOS.

References

1. GCOS. Available online: https://www.wmo.int/pages/prog/gcos/Publications/gcos-154.pdf (accessed on 23 November).
2. Porporato, A.; Daly, E.; Rodriguez-Iturbe, I. Soil water balance and ecosystem response to climate change. *Am. Naturalist* **2004**, *164*, 625–632.
3. Vereecken, H.; Huisman, J.; Pachepsky, Y.; Montzka, C.; van der Kruk, J.; Bogena, H.; Weihermüller, L.; Herbst, M.; Martinez, G.; Vanderborght, J. On the spatio-temporal dynamics of soil moisture at the field scale. *J. Hydrol.* **2014**, *516*, 76–96.
4. Seneviratne, S.I.; Corti, T.; Davin, E.L.; Hirschi, M.; Jaeger, E.B.; Lehner, I.; Orlowsky, B.; Teuling, A.J. Investigating soil moisture–climate interactions in a changing climate: A review. *Earth-Sci. Rev.* **2010**, *99*, 125–161.

5. Loew, A.; Holmes, T.; de Jeu, R. The european heat wave 2003: Early indicators from multisensoral microwave remote sensing? *J. Geophys. Res.: Atmos. (1984–2012)* **2009**, *114*, doi:10.1029/2008JD010533.
6. Wagner, W.; Naeimi, V.; Scipal, K.; de Jeu, R.; Martínez-Fernández, J. Soil moisture from operational meteorological satellites. *Hydrogeol. J.* **2007**, *15*, 121–131.
7. Loew, A.; Ludwig, R.; Mauser, W. Derivation of surface soil moisture from envisat asar wide swath and image mode data in agricultural areas. *IEEE Trans. Geosci. Remote Sens.* **2006**, *44*, 889–899.
8. Njoku, E.G.; Entekhabi, D. Passive microwave remote sensing of soil moisture. *J. Hydrol.* **1996**, *184*, 101–129.
9. Owe, M.; de Jeu, R.; Holmes, T. Multisensor historical climatology of satellite-derived global land surface moisture. *J. Geophys. Res. Earth Surf.* **2008**, *113*, F01002.
10. Naeimi, V.; Scipal, K.; Bartalis, Z.; Hasenauer, S.; Wagner, W. An improved soil moisture retrieval algorithm for ERS and METOP scatterometer observations. *IEEE Trans. Geosci. Remote Sens.* **2009**, *47*, 1999–2013.
11. Wagner, W.; Lemoine, G.; Rott, H. A method for estimating soil moisture from ERS scatterometer and soil data. *Remote Sens. Environ.* **1999**, *70*, 191–207.
12. Kerr, Y.H.; Waldteufel, P.; Wigneron, J.P.; Martinuzzi, J.; Font, J.; Berger, M. Soil moisture retrieval from space: The soil moisture and ocean salinity (SMOS) mission. *IEEE Trans. Geosci. Remote Sens.* **2001**, *39*, 1729–1735.
13. Liu, Y.Y.; Parinussa, R.M.; Dorigo, W.A.; de Jeu, R.A.M.; Wagner, W.; van Dijk, A.I.J.M.; McCabe, M.F.; Evans, J.P. Developing an improved soil moisture dataset by blending passive and active microwave satellite-based retrievals. *Hydrol. Earth Syst.Sci.* **2011**, *15*, 425–436.
14. Wagner, W.; Dorigo, W.; de Jeu, R.; Fernandez, D.; Benveniste, J.; Haas, E.; Ertl, M. Fusion of active and passive microwave observations to create an essential climate variable data record on soil moisture. *ISPRS Ann. Photogramm. Remote Sens. Spat. Inf. Sci.* **2012**, *I-7*, 315–321.
15. Dorigo, W.A.; Gruber, A.; de Jeu, R.A.M.; Wagner, W.; Stacke, T.; Loew, A.; Albergel, C.; Brocca, L.; Chung, D.; Parinussa, R.M.; *et al.* Evaluation of the ESA CCI soil moisture product using ground-based observations. *Remote Sens. Environ.* **2015**, *162*, 380–395.
16. Albergel, C.; Rüdiger, C.; Carrer, D.; Calvet, J.-C.; Fritz, N.; Naeimi, V.; Bartalis, Z.; Hasenauer, S. An evaluation of ascat surface soil moisture products with *in situ* observations in southwestern france. *Hydrol. Earth Syst. Sci.* **2009**, *13*, 115–124.
17. Brocca, L.; Hasenauer, S.; Lacava, T.; Melone, F.; Moramarco, T.; Wagner, W.; Dorigo, W.; Matgen, P.; Martínez-Fernández, J.; Llorens, P.; *et al.* Soil moisture estimation through ASCAT and AMSR-E sensors: An intercomparison and validation study across europe. *Remote Sens. Environ.* **2011**, *115*, 3390–3408.
18. Sánchez, N.; Martínez-Fernández, J.; Scaini, A.; Pérez-Gutiérrez, C. Validation of the SMOS l2 soil moisture data in the remedhus network (Spain). *IEEE Trans. Geosci. Remote Sens.* **2012**, *50*, 1602–1611.
19. Fascetti, F.; Pierdicca, N.; Pulvirenti, L.; Crapolicchio, R.; Muñoz-Sabater, J. A comparison of ASCAT and SMOS soil moisture retrievals over europe and northern africa from 2010 to 2013. *Int. J. Appl. Earth Obs. Geoinf.* **2015**, in press.
20. Draper, C.S.; Walker, J.P.; Steinle, P.J.; de Jeu, R.A.; Holmes, T.R. An evaluation of AMSR–E derived soil moisture over australia. *Remote Sens. Environ.* **2009**, *113*, 703–710.

21. Su, C.-H.; Ryu, D.; Young, R.I.; Western, A.W.; Wagner, W. Inter-comparison of microwave satellite soil moisture retrievals over the murrumbidgee basin, southeast Australia. *Remote Sens. Environ.* **2013**, *134*, 1–11.
22. Gruhier, C.; Rosnay, P.D.; Hasenauer, S.; Holmes, T.; Jeu, R.D.; Kerr, Y.; Mougin, E.; Njoku, E.; Timouk, F.; Wagner, W. Soil moisture active and passive microwave products: Intercomparison and evaluation over a Sahelian site. *Hydrol. Earth Syst. Sci.* **2010**, *14*, 141–156.
23. Louvet, S.; Pellarin, T.; al Bitar, A.; Cappelaere, B.; Galle, S.; Grippa, M.; Gruhier, C.; Kerr, Y.; Lebel, T.; Mialon, A.; *et al.* SMOS soil moisture product evaluation over West-Africa from local to regional scale. *Remote Sens. Environ.* **2015**, *156*, 383–394.
24. Al Bitar, A.; Leroux, D.; Kerr, Y.H.; Merlin, O.; Richaume, P.; Sahoo, A.; Wood, E.F. Evaluation of SMOS soil moisture products over continental US using the SCAN/SNOTEL network. *IEEE Trans. Geosci. Remote Sens.* **2012**, *50*, 1572–1586.
25. Collow, T.W.; Robock, A.; Basara, J.B.; Illston, B.G. Evaluation of SMOS retrievals of soil moisture over the central United States with currently available *in situ* observations. *J. Geophys. Res. Atmos.* **2012**, *117*, doi:10.1029/2011JD017095.
26. Al-Yaari, A.; Wigneron, J.P.; Ducharne, A.; Kerr, Y.; de Rosnay, P.; de Jeu, R.; Govind, A.; Al Bitar, A.; Albergel, C.; Muñoz-Sabater, J.; *et al.* Global-scale evaluation of two satellite-based passive microwave soil moisture datasets (SMOS and AMSR-E) with respect to land data assimilation system estimates. *Remote Sens. Environ.* **2014**, *149*, 181–195.
27. Albergel, C.; Dorigo, W.; Reichle, R.H.; Balsamo, G.; de Rosnay, P.; Muñoz-Sabater, J.; Isaksen, L.; de Jeu, R.; Wagner, W. Skill and global trend analysis of soil moisture from reanalyses and microwave remote sensing. *J. Hydrometeorol.* **2013**, *14*, 1259–1277.
28. Long, D.; Shen, Y.; Sun, A.; Hong, Y.; Longuevergne, L.; Yang, Y.; Li, B.; Chen, L. Drought and flood monitoring for a large karst plateau in southwest China using extended grace data. *Remote Sens. Environ.* **2014**, *155*, 145–160.
29. Xu, K.; Yang, D.; Xu, X.; Lei, H. Copula based drought frequency analysis considering the spatio-temporal variability in southwest China. *J. Hydrol.* **2015**, *527*, 630–640.
30. Qiu, J. China drought highlights future climate threats. *Nature* **2010**, *465*, 142–143.
31. Fan, Z.-X.; Bräuning, A.; Thomas, A.; Li, J.-B.; Cao, K.-F. Spatial and temporal temperature trends on the Yunnan plateau (southwest China) during 1961–2004. *Int. J. Climatol.* **2011**, *31*, 2078–2090.
32. Li, Y.-G.; He, D.; Hu, J.-M.; Cao, J. Variability of extreme precipitation over Yunnan province, China 1960–2012. *Int. J. Climatol.* **2015**, *35*, 245–258.
33. Abbas, S.; Nichol, J.; Qamer, F.; Xu, J. Characterization of drought development through remote sensing: A case study in central Yunnan, china. *Remote Sens.* **2014**, *6*, 4998–5018.
34. Yang, J.; Gong, D.; Wang, W.; Hu, M.; Mao, R. Extreme drought event of 2009/2010 over southwestern China. *Meteorol. Atmos. Phys.* **2012**, *115*, 173–184.
35. Zhang, L.; Xiao, J.; Li, J.; Wang, K.; Lei, L.; Guo, H. The 2010 spring drought reduced primary productivity in southwestern China. *Environ. Res. Lett.* **2012**, *7*, 045706.
36. Njoku, E.G.; Jackson, T.J.; Lakshmi, V.; Chan, T.K.; Nghiem, S.V. Soil moisture retrieval from AMSR-E. *IEEE Trans. Geosci. Remote Sens.* **2003**, *41*, 215–229.
37. Rebel, K.T.; de Jeu, R.A.M.; Ciais, P.; Viovy, N. A global analysis of soil moisture derived from satellite observations and a land surface model. *Hydrol. Earth Syst. Sci.* **2012**, *16*, 833–847.

38. Lei, F.; Crow, W.; Shen, H.; Parinussa, R.; Holmes, T. The impact of local acquisition time on the accuracy of microwave surface soil moisture retrievals over the contiguous United States. *Remote Sens.* **2015**, *7*, 13448–13465.
39. Figa-Saldaña, J.; Wilson, J.J.; Attema, E.; Gelsthorpe, R.; Drinkwater, M.; Stoffelen, A. The advanced scatterometer (ASCAT) on the meteorological operational (METOP) platform: A follow on for European wind scatterometers. *Can. J. Remote Sens.* **2002**, *28*, 404–412.
40. Wagner, W.; Bloeschl, G.; Pampaloni, P.; Calvet, J.-C.; Bizzarri, B.; Wigneron, J.-P.; Kerr, Y. Operational readiness of microwave remote sensing of soil moisture for hydrologic applications. *Nord. Hydrol.* **2007**, *38*, 1–20.
41. Reynolds, C.A.; Jackson, T.J.; Rawls, W.J. Estimating soil water-holding capacities by linking the food and agriculture organization soil map of the world with global pedon databases and continuous pedotransfer functions. *Water Resour. Res.* **2000**, *36*, 3653–3662.
42. Hollmann, R.; Merchant, C.J.; Saunders, R.; Downy, C.; Buchwitz, M.; Cazenave, A.; Chuvieco, E.; Defourny, P.; de Leeuw, G.; Forsberg, R.; *et al.* The ESA climate change initiative: Satellite data records for essential climate variables. *Bull. Am. Meteorol. Soc.* **2013**, *94*, 1541–1552.
43. Liu, Y.Y.; Dorigo, W.A.; Parinussa, R.M.; de Jeu, R.A.M.; Wagner, W.; McCabe, M.F.; Evans, J.P.; van Dijk, A.I.J.M. Trend-preserving blending of passive and active microwave soil moisture retrievals. *Remote Sens. Environ.* **2012**, *123*, 280–297.
44. Kerr, Y.H.; Waldteufel, P.; Wigneron, J.-P.; Delwart, S.; Cabot, F.O.; Boutin, J.; Escorihuela, M.-J.; Font, J.; Reul, N.; Gruhier, C. The SMOS mission: New tool for monitoring key elements ofthe global water cycle. *IEEE Proc.* **2010**, *98*, 666–687.
45. Wigneron, J.-P.; Kerr, Y.; Waldteufel, P.; Saleh, K.; Escorihuela, M.-J.; Richaume, P.; Ferrazzoli, P.; de Rosnay, P.; Gurney, R.; Calvet, J.-C. L-band microwave emission of the biosphere (L-MEB) model: Description and calibration against experimental data sets over crop fields. *Remote Sens. Environ.* **2007**, *107*, 639–655.
46. Kerr, Y.H.; Waldteufel, P.; Richaume, P.; Wigneron, J.P.; Ferrazzoli, P.; Mahmoodi, A.; Al Bitar, A.; Cabot, F.; Gruhier, C.; Juglea, S.E. The SMOS soil moisture retrieval algorithm. *IEEE Trans. Geosci. Remote Sens.* **2012**, *50*, 1384–1403.
47. Al-Yaari, A.; Wigneron, J.P.; Ducharne, A.; Kerr, Y.H.; Wagner, W.; de Lannoy, G.; Reichle, R.; Al Bitar, A.; Dorigo, W.; Richaume, P.; *et al.* Global-scale comparison of passive (SMOS) and active (ASCAT) satellite based microwave soil moisture retrievals with soil moisture simulations (Merra-Land). *Remote Sens. Environ.* **2014**, *152*, 614–626.
48. Dee, D.P.; Uppala, S.M.; Simmons, A.J.; Berrisford, P.; Poli, P.; Kobayashi, S.; Andrae, U.; Balmaseda, M.A.; Balsamo, G.; Bauer, P.; *et al.* The Era-interim reanalysis: Configuration and performance of the data assimilation system. *Q. J. R. Meteorol. Soc.* **2011**, *137*, 553–597.
49. Kummerow, C.; Simpson, J.; Thiele, O.; Barnes, W.; Chang, A.T.C.; Stocker, E.; Adler, R.F.; Hou, A.; Kakar, R.; Wentz, F.; *et al.* The status of the tropical rainfall measuring mission (TRMM) after two years in orbit. *J. Appl. Meteorol.* **2000**, *39*, 1965–1982.
50. Iguchi, T.; Kozu, T.; Meneghini, R.; Awaka, J.; Okamoto, K.I. Rain-profiling algorithm for the TRMM precipitation radar. *J. Appl. Meteorol.* **2000**, *39*, 2038–2052.
51. Willmott, C.J. Some comments on the evaluation of model performance. *Bull. Am. Meteorol. Soc.* **1982**, *63*, 1309–1313.

52. Entekhabi, D.; Reichle, R.H.; Koster, R.D.; Crow, W.T. Performance metrics for soil moisture retrievals and application requirements. *J. Hydrometeorol.* **2010**, *11*, 832–840.
53. Scipal, K.; Drusch, M.; Wagner, W. Assimilation of a ERS scatterometer derived soil moisture index in the ECMWF numerical weather prediction system. *Adv. Water Resour.* **2008**, *31*, 1101–1112.
54. Jackson, T.J.; Cosh, M.H.; Bindlish, R.; Starks, P.J.; Bosch, D.D.; Seyfried, M.; Goodrich, D.C.; Moran, M.S.; Jinyang, D. Validation of advanced microwave scanning radiometer soil moisture products. *IEEE Trans. Geosci. Remote Sens.* **2010**, *48*, 4256–4272.
55. Saleh, K.; Wigneron, J.-P.; de Rosnay, P.; Calvet, J.-C.; Escorihuela, M.J.; Kerr, Y.; Waldteufel, P. Impact of rain interception by vegetation and mulch on the L-band emission of natural grass. *Remote Sens. Environ.* **2006**, *101*, 127–139.
56. Rowlandson, T.L.; Hornbuckle, B.K.; Bramer, L.M.; Patton, J.C.; Logsdon, S.D. Comparisons of evening and morning SMOS passes over the Midwest United States. *IEEE Trans. Geosci. Remote Sens.* **2012**, *50*, 1544–1555.
57. Griesfeller, A.; Lahoz, W.A.; Jeu, R.A.M.D.; Dorigo, W.; Haugen, L.E.; Svendby, T.M.; Wagner, W. Evaluation of satellite soil moisture products over Norway using ground-based observations. *Int. J. Appl. Earth Obs. Geoinf.* **2015**, in press.
58. Cho, E.; Choi, M.; Wagner, W. An assessment of remotely sensed surface and root zone soil moisture through active and passive sensors in northeast Asia. *Remote Sens. Environ.* **2015**, *160*, 166–179.
59. Zeng, J.; Li, Z.; Chen, Q.; Bi, H.; Qiu, J.; Zou, P. Evaluation of remotely sensed and reanalysis soil moisture products over the Tibetan plateau using *in situ* observations. *Remote Sens. Environ.* **2015**, *163*, 91–110.
60. Su, Z.; Rosnay, P.; Wen, J.; Wang, L.; Zeng, Y. Evaluation of ecmwf's soil moisture analyses using observations on the Tibetan plateau. *J. Geophys. Res. Atmos.* **2013**, *118*, 5304–5318.
61. Pratola, C.; Barrett, B.; Gruber, A.; Kiely, G.; Dwyer, E. Evaluation of a global soil moisture product from finer spatial resolution sar data and ground measurements at Irish sites. *Remote Sens.* **2014**, *6*, 8190–8219.
62. Peng, J.; Niesel, J.; Loew, A. Evaluation of soil moisture downscaling using a simple thermal based proxy—The remedhus network (Spain) example. *Hydrol. Earth Syst. Sci. Discuss.* **2015**, *12*, 8505–8551.
63. Oliva, R.; Daganzo, E.; Kerr, Y.H.; Mecklenburg, S.; Nieto, S.; Richaume, P.; Gruhier, C. SMOS radio frequency interference scenario: Status and actions taken to improve the RFI environment in the 1400–1427-MHZ passive band. *IEEE Trans. Geosci. Remote Sens.* **2012**, *50*, 1427–1439.
64. Piles, M.; Camps, A.; Vall-llossera, M.; Corbella, I.; Panciera, R.; Rudiger, C.; Kerr, Y.H.; Walker, J. Downscaling SMOS-derived soil moisture using modis visible/infrared data. *IEEE Trans. Geosci. Remote Sens.* **2011**, *49*, 3156–3166.
65. Peng, J.; Loew, A.; Zhang, S.; Wang, J.; Niesel, J. Spatial downscaling of satellite soil moisture data using a vegetation temperature condition index. *IEEE Trans. Geosci. Remote Sens.* **2016**, *54*, 558–566.

© 2015 by the authors; licensee MDPI, Basel, Switzerland. This article is an open access article distributed under the terms and conditions of the Creative Commons Attribution license (http://creativecommons.org/licenses/by/4.0/).